Demistify: an LES and SCM intercomparison of radiation fog

Ian Boutle[1], Wayne Angevine[2], Jian-Wen Bao[3], Thierry Bergot[4], Ritthik Bhattacharya[5], Andreas Bott[6], Leo Ducongé[4], Richard Forbes[7], Tobias Goecke[8], Evelyn Grell[9], Adrian Hill[1], Adele Igel[10], Innocent Kudzotsa[11], Christine Lac[4], Bjorn Maronga[12], Sami Romakkaniemi[11], Juerg Schmidli[5], Johannes Schwenkel[12], Gert-Jan Steeneveld[13], and Benoît Vié[4]

[1]Met Office, Exeter, UK
[2]CIRES, University of Colorado, and NOAA Chemical Sciences Laboratory, Boulder, USA
[3]NOAA Physical Sciences Laboratory, Boulder, USA
[4]CNRM, Université de Toulouse, Météo-France, CNRS, Toulouse, France
[5]University of Frankfurt, Germany
[6]University of Bonn, Germany
[7]ECMWF, Reading, UK
[8]DWD, Offenbach, Germany
[9]CIRES, University of Colorado, and NOAA Physical Sciences Laboratory, Boulder, USA
[10]UC Davis, USA
[11]FMI, Kuopio, Finland
[12]University of Hannover, Germany
[13]Wageningen University, Netherlands

Correspondence: I. A. Boutle (ian.boutle@metoffice.gov.uk)

Abstract. An intercomparison between 10 single-column (SCM) and 5 large-eddy simulation (LES) models is presented for a radiation fog case study inspired by the LAN-FEX field campaign. 7 of the SCMs represent single-column equivalents of operational numerical weather prediction (NWP) models, whilst 3 are research-grade SCMs designed for fog simulation, and the LES are designed to reproduce in the best manner currently possible the underlying physical processes governing fog formation. The LES model results are of variable quality, and do not provide a consistent baseline against which to compare the NWP models, particularly under high aerosol or cloud droplet number concentration (CDNC) conditions. The main SCM bias appears to be toward over-development of fog, i.e. fog which is too thick, although the inter-model variability is large. In reality there is a subtle balance between water lost to the surface and water condensed into fog, and the ability of a model to accurately simulate this process strongly determines the quality of its forecast. Some NWP-SCMs do not represent fundamental components of this process (e.g. cloud droplet sedimentation) and therefore are naturally hampered in their ability to deliver accurate simulations. Finally, we show that modelled fog development is as sensitive to the shape of the cloud droplet size distribution, a rarely studied or modified part of the microphysical parametrization, as it is to the underlying aerosol or CDNC.

1 Introduction

Most operational numerical weather prediction (NWP) centres will list errors in fog forecasting amongst their top model problems, with the requirement for improvement considered high-priority (Hewson, 2019). The key customer driving this is the aviation sector, with ≈40% of all delays (≈50% of weather related delays) at busy airports (such as London Heathrow, Paris CDG, San Francisco and New Delhi) being due to low visibility events. In the best case, these delays are inconvenient for passengers and expensive for airline operators (Cook and Tanner, 2015; Kulkarni et al., 2019). However, in the worst case, fog can also be a significant danger and is the second most likely cause of weather related accidents (Gultepe et al., 2019; Leung et al., 2020).

Despite this importance, there is no international community working together on improving fog modelling. The Global Atmospheric System Studies (GASS) panel facilitates projects which draw together researchers from around the globe to work on specific and targeted process studies. Utilising large-eddy simulation (LES) and single-column (SCM) versions of NWP models, previous projects (including under GABLS and GCSS) have made significant advances in the understanding and modelling of stable boundary layers (Beare et al., 2006; Cuxart et al., 2006), turbulent clouds (van der Dussen et al., 2013; Neggers et al., 2017) and aerosol-cloud interactions (Hill et al., 2015). A new GASS project related to fog modelling therefore presents an opportunity to form a community and address the challenges together, building on the previous understanding of the multitude of processes at play in radiation fog.

A previous intercomparison of radiation fog in SCM models (Bergot et al., 2007) demonstrated that even before fog onset there were considerable differences between models, and found the model skill to be low. The current intercomparison considers a new generation of NWP-SCM models, with more complex physical parametrizations, and for the first time will compare LES models for the same radiation fog event. The key questions to be considered include:

- How well can models simulate the development of radiation fog?

- What are the key processes governing the development of radiation fog, i.e. aerosol, cloud microphysics, radiation, turbulence, dew deposition, something else?

- Which of these processes are mostly responsible for the biases seen in current NWP models?

- What level of complexity is required from NWP models to adequately simulate these processes?

The initial phase of work, documented in this paper, will constrain the surface properties and focus primarily on the atmospheric development of fog. This will document the current state of LES and NWP fog modelling within the community, and provide guidance on opportunities for improvements applicable to many models. Further stages of the project will then consider feedbacks through the land surface, more complicated cases with non-local forcing, and the representation of fog in climate models, something which has rarely been looked at in the literature.

2   Intercomparison design and participants

The first intensive observational period (IOP1) of the Local and Non-local Fog Experiment (LANFEX, Price et al., 2018) presented a relatively simple case of fog forming in a nocturnal stable boundary layer, developing over several hours into turbulent, optically-thick fog. However, NWP modelling of this event (Boutle et al., 2018) showed significant errors in the structure and evolution of the fog. Therefore we base the intercomparison around a slightly idealised version of IOP1. The case is based at the Met Office observational site at Cardington, UK (52.1015N, 0.4159W) and occurred on the night of 24-25 November 2014. Models are initialised from the 17 UTC radiosonde profile and forced throughout the night by the observed surface skin temperature (measured with an infra-red radiation thermometer, Price et al., 2018). No other forcing is used, to keep the case simple and allow for maximum participation amongst modelling centres. This makes the case identical to the LES case presented in Boutle et al. (2018), which showed good agreement with a 3D NWP model, and testing has shown little difference to SCM results from applying advective forcing derived from the radiosondes (not shown). Forcing with surface temperature also constrains the problem to an atmospheric one, focussing on the cloud, radiation and turbulence interaction. In reality, patchy fog began to form around 18 UTC, with persistent fog and visibilities around 100 m from 20 UTC for 12 hours before clearance. The real clearance was driven by a bank of overlying cloud cover arriving at the site, which we do not attempt to represent in the simplified case.

Because of the sensitivity to cloud and aerosol processes previously discussed in Boutle et al. (2018), we request two simulations from all participants. For models which do not represent aerosol processing, the cloud droplet number concentration (CDNC) should be prescribed (if possible) as:

- c10: fixed cloud droplet number concentration of $10\,\mathrm{cm^{-3}}$,

- c50: fixed cloud droplet number concentration of $50\,\mathrm{cm^{-3}}$,

For models which do represent aerosol processing, the accumulation mode aerosol should be prescribed as:

- a100: initial accumulation mode (0.15 μm diameter, σ=2) aerosol of $100\,\mathrm{cm^{-3}}$,

- a650: initial accumulation mode (0.15 μm diameter, σ=2) aerosol of $650\,\mathrm{cm^{-3}}$.

Experiments c10 and a100 will be referred to as "low" aerosol/CDNC simulations, whilst c50 and a650 will be referred to as "high" aerosol/CDNC simulations. The aerosol setup is complicated slightly, as some of the more sophisticated aerosol processing models also require specification of the Aitken and coarse mode aerosols, which are prescribed (as in Boutle et al., 2018) as $1000\,\mathrm{cm^{-3}}$ with mean diameter 0.05 μm and $2\,\mathrm{cm^{-3}}$ with mean diameter 1 μm. Vié et al. (2021) discuss how it is only really sensible to impose these additional aerosols in models which represent prognostic supersaturation of liquid water, otherwise excessive activation of the Aitken mode aerosol into cloud droplets occurs.

Although the surface temperature is specified, many models still require some parametrization of the surface characteristics (to estimate the turbulent fluxes into the atmosphere), which is set as a flat, homogeneous, grass surface with the following parameters:

- Momentum roughness length (z_{0m}): 0.1 m,

- Heat roughness length (z_{0h}): 0.001 m,

- Leaf area index: 2,

- Albedo: 0.25,

- Emissivity: 0.98.

This setup is derived from the characteristics of the Cardington site (Price et al., 2018). Evapotranspiration should be unrestricted (i.e. like a sea-surface), to avoid complexities associated with soil moisture and land-surface models, although in practice the observed fluxes are into the surface for most of the night and so this simplification should be of limited importance if the models can reproduce this behaviour.

Table 1 shows the model configurations that have been submitted and are analysed in this paper, whilst Tables 2 and 3 give some further relevant details about the setups of the LES and SCM models respectively.

3 Results

3.1 Liquid water path evolution

Figure 1 presents an initial view of the submitted models, separated by their class (LES or SCM) and aerosol or CDNC (low or high). As there is no higher-level cloud in any of the simulations, any non-zero liquid water path is attributable to fog. This is consistent with the observations until 08 UTC, when the upper level cloud arrived at the site, and is responsible for the sharp increase in LWP after this time (which should not be reproduced by the simulations). The first thing to note is that all models do at least form fog, but beyond this there is very little consistency between models.

The observations are most consistent with the low aerosol/CDNC setup. For the SCM runs, only MiFog, Meso-NH, UM and d91 have liquid water path (LWP) evolution in line with the observations, although PaFog, IFS and WRF are only just outside the observational range. The other models considerably over-estimate the LWP. In general, the LES runs are in closer agreement with each other and the observations, but considerable spread exists between them for the high aerosol/CDNC runs. With the exception of ICON and FV3-GFS (which does not represent variable CDNC), all models show substantial variation between the low and high aerosol/CDNC setups, producing higher LWP with greater aerosol/CDNC.

To first order, the most important factor in determining the LWP evolution of all models is the rate at which water is deposited from the atmosphere to the surface. The observations (see Boutle et al., 2018, Fig 4a) are broadly constant at around 20 $\mathrm{gm^{-2}hr^{-1}}$ throughout the night, and most models achieve this value despite the wildly varying LWP (possibly because the water deposition is constrained by the longwave cooling of the atmosphere). Because the water deposition rate is strongly affected by the LWP, we must therefore normalise it before comparing the models, which is shown in Figure 2. This shows a clear link between the deposition rate and LWP – models which do not deposit enough water onto the surface end up with LWP values which are too high, and models which deposit too much water onto the surface end up with LWP values which are too low.

The reasons for the varying water deposition rate are very model dependent, although we can try to summarise some consistent themes in the SCMs:

- Models which do not represent cloud droplet sedimentation – these models (FV3-GFS, COSMO, IFS) are significantly hampered by their lack of this process, which is likely to be the dominant mechanism of water removal in reality. IFS is able to compensate to a certain extent by autoconverting significant amounts of fog into precipitation and removing it that way, which explains its lower LWP than COSMO or FV3-GFS which are unable to do this. Improvements here should be easy to achieve via modifications to the microphysical parametrization.

- Models which produce excessive positive surface latent heat flux (Fig. 5) – these models (WRF, COSMO) will always struggle to deposit enough water through microphysical processes because it is being constantly replenished via evaporation from the surface. Understanding the mechanisms behind this error can be tricky, as it may not simply be an issue with the turbulent exchange parametrizations, but could also be a feedback. For example, as discussed in Boutle et al. (2018), forming fog which is slightly too optically thick can drive an erroneous positive flux, which in turn leads to further development of thicker fog.

- The precise nature of the microphysical parametrizations responsible for water deposition – even models which represent all processes and maintain a low latent heat flux (ICON, UM, Meso-NH) can have large discrepancies because of how the different water deposition rates feed back onto model evolution. This suggests that more work is required on the basic observations, understanding and modelling of water deposition. For example Meso-NH is the only model to represent turbulent deposition of droplets in addition to sedimentation, giving it one of the highest deposition rates.

The LES models may be closer in their behaviour, but still show some similar traits to the SCMs. In particular, the models with the highest deposition rates tend to have the lowest

Institution	Model	Type	Experiments submitted	Lead participant	Reference
Bonn University	MiFog	SCM	a100, a650	Andreas Bott	Bott et al. (1990)
Bonn University	PaFog	SCM	a100, a650	Andreas Bott	Bott and Trautmann (2002)
CIRES/NOAA	WRF	SCM*	c10, c50, a100, a650	Wayne Angevine	Angevine et al. (2018)
UC Davis	RAMS	LES	c10, c50, a100, a650	Adele Igel	Cotton et al. (2003)
DWD	ICON	SCM*	c10, c50	Tobias Goecke	Bašták Ďurán et al. (2021)
ECMWF	IFS	SCM*	c10, c50	Richard Forbes	Ahlgrimm and Forbes (2014)
FMI	UCLA-SALSA	LES	a100, a650	Innocent Kudzotsa	Tonttila et al. (2017)
Frankfurt University	COSMO	SCM*	c10, c50	Ritthik Bhattacharya	Baldauf et al. (2011)
Hannover University	PALM	LES	a100, a650	Johannes Schwenkel	Maronga et al. (2020)
Met Office	Unified Model	SCM*	c10, c50	Ian Boutle	Bush et al. (2020)
Met Office	MONC	LES	c10, c50, a100, a650	Adrian Hill	Dearden et al. (2018)
Meteo France	Meso-NH	SCM*	c10, c50, a100, a650	Leo Ducongé	Lac et al. (2018)
Meteo France	Meso-NH	LES	c10, c50, a100, a650	Leo Ducongé	Lac et al. (2018)
NOAA	FV3-GFS	SCM*	c300	Evelyn Grell	Firl et al. (2020)
Wageningen University	d91	SCM	c10, c50	Gert-Jan Steeneveld	Duynkerke (1991)

Table 1. Modelling centres, lead participants, models and model simulations submitted. * denotes the SCMs that have the physics package and vertical resolution of operational NWP models.

Model	Grid-length (dx, dz)	Aerosol processing	Microphysics type	Prognostic supersaturation	Cloud droplet settling	Subgrid turbulence
RAMS	4 m, 1.5 m	Accumulation	Bulk	N	Y	TKE
UCLA-SALSA	4 m, 1.5 m	Full	Bin	Y	Y	Smagorinsky
PALM	1.5 m, 1.5 m	Accumulation	Bulk	N	Y	TKE
MONC	4 m, 1.5 m	Accumulation	Bulk	N	Y	Smagorinsky
Meso-NH	4 m, 1.5 m	Accumulation	Bulk	N	Y	TKE

Table 2. LES model details: horizontal (dx) and vertical (dz) grid-length, type of aerosol processing, microphysics parametrization details and type of subgrid turbulence scheme (TKE=Turbulent kinetic energy closure).

Model	Grid-length (lowest level, levels below 150 m)	Aerosol processing	Microphysics type	Prognostic supersaturation	Cloud droplet settling	Subgrid turbulence
MiFog	0.5 m, 61	Full	Bin	Y	Y	TKE
PaFog	0.5 m, 61	Full	Bulk	Y	Y	TKE
WRF	12 m, 6	Accumulation	Bulk	N	Y	TKE+EDMF
ICON	10 m, 3	None	Bulk	N	Y	TKE
IFS	10 m, 6	None	Bulk	N	N	EDMF
COSMO	10 m, 7	None	Bulk	N	N	TKE*
Unified Model	2.5 m, 6	None	Bulk	N	Y	K1+NL
Meso-NH	5 m, 7	Accumulation	Bulk	N	Y	TKE
FV3-GFS	21 m, 3	None	Bulk	N	N	EDMF
d91	3.3 m, 27	None	Bulk	N	Y	K1

Table 3. SCM model details: height of lowest model level and number of levels below 150 m, type of aerosol processing, microphysics parametrization details and type of subgrid turbulence scheme (EDMF=Eddy-diffusivity mass-flux closure, K1=local first order closure, NL=non-local/counter-gradient transport, *modified for SCM as in Buzzi et al. (2011)).
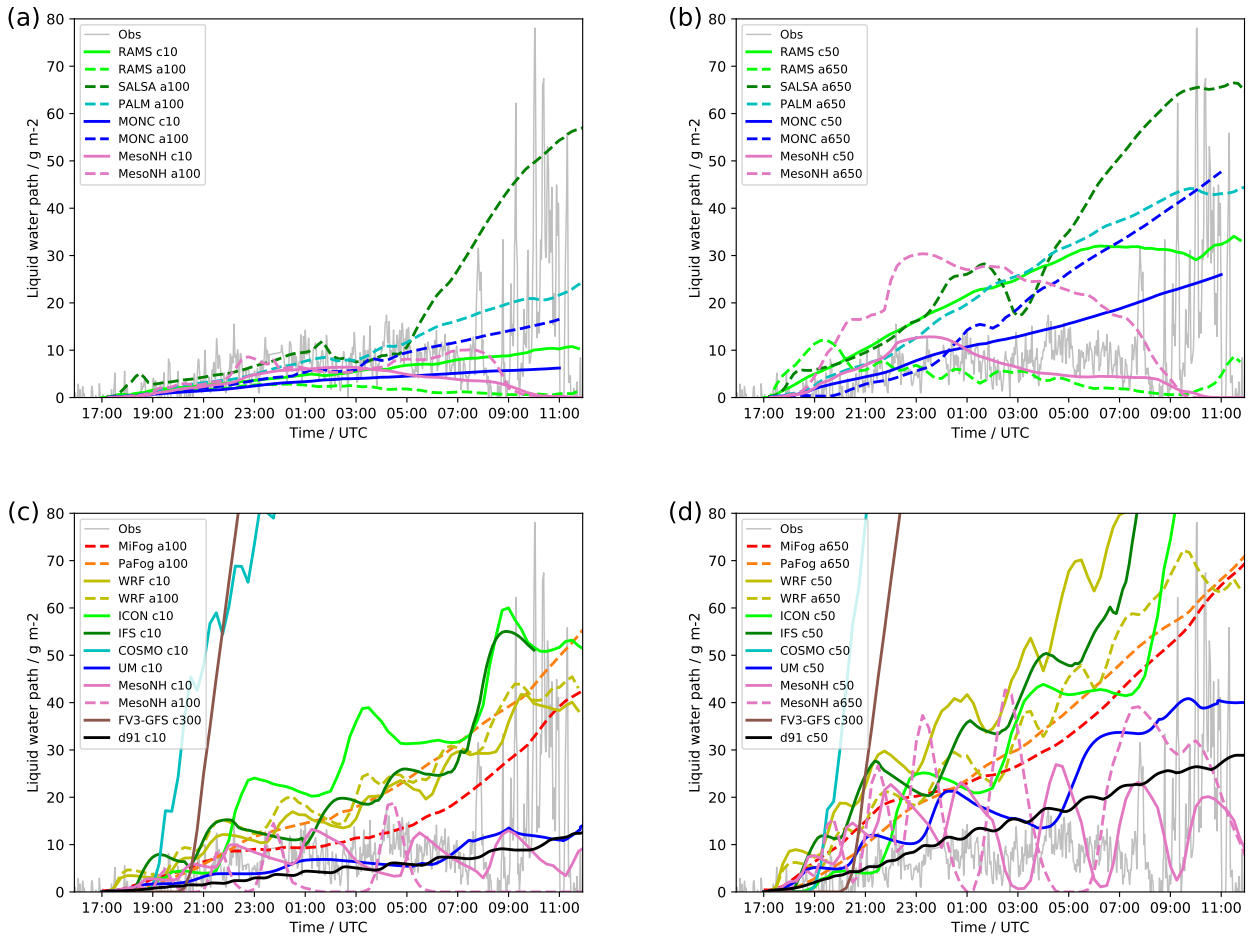
Figure 1. Liquid water path observed and modelled by (a) low aerosol/CDNC LES, (b) high aerosol/CDNC LES, (c) low aerosol/CDNC SCMs and (d) high aerosol/CDNC SCMs.

LWP, and visa-versa. However, the mechanism by which this is achieved can be considerably different between the models. RAMS-c10 for example has a significant positive latent heat flux, which is balanced by a larger cloud droplet sedimentation rate than any other LES, to give an overall water deposition rate and LWP comparable to the other models. Differences like this show why it is difficult to use the LES as process models, because although they are producing more consistent behaviour, the processes by which they achieve it are not consistent.

The one LES (and indeed SCM) model which doesn't appear to follow the pattern is Meso-NH-c10, which has one of the highest water deposition rates of any of the models, yet manages to achieve a reasonable fog simulation in all cases. This arises because it simulates a very low effective radius (Fig 3), resulting in very strong absorption and emission from the fog layer, helping the fog to grow despite the high water deposition. The reason for the low effective radius appears to be the use of the Martin et al. (1994) parametrization

with a default 'land' setup, i.e. it is using a high ($300\,\mathrm{cm}^{-3}$) assumed CDNC value in the effective radius parametrization, rather than the actual CDNC used by the microphysical parametrization. The Meso-NH-a100 simulation, which has a consistent link between cloud droplet number and effective radius, shows a response more consistent with the other models. This highlights the importance of using consistent assumptions between radiation and microphysical parametrizations.

The RAMS-a100 simulation has almost the opposite effect, with a high effective radius resulting in a very low LWP. This however arises because the model rapidly depletes all of the aerosol in the atmosphere, and therefore has nothing to activate into cloud droplets. As a consequence, after the initial fog formation, no new small droplets are formed, but the droplets which do exist grow in size and sediment out, resulting in a very low liquid water path. This is particularly noticeable in the RAMS-a650 simulation, which has the lowest LWP of any model in the 'high' experiment. Figure 4(b)
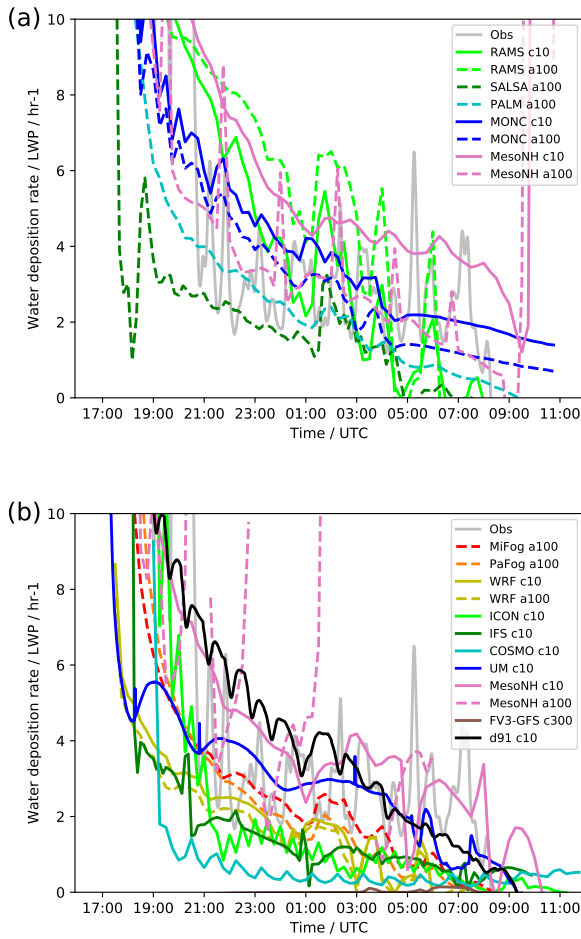
Figure 2. Water deposition rate divided by liquid water path observed and modelled by (a) low aerosol/CDNC LES, (b) low aerosol/CDNC SCMs.
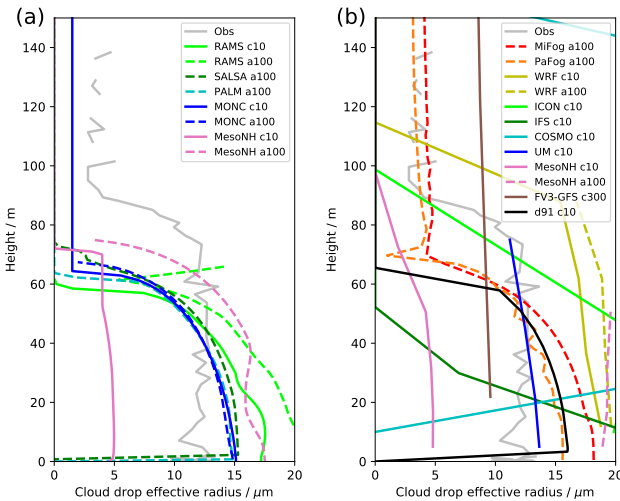
Figure 3. Effective radius observed and simulated by the low aerosol/CDNC (a) LES, and (b) SCMs, at 00 UTC.

shows that this is linked to a very low CDNC, despite the high initial aerosol concentration, because most of the aerosol has been depleted. Fig. 4(b) also shows an interesting clustering between the full aerosol processing models, which predict CDNC values in the range 40-60 cm^{-3}, and the accumulation only models which predict CDNC values in the range 70-90 cm^{-3}. This shows that even though the latter group are only considering a subset of the full aerosol distribution, they may still be over-estimating the activation occurring in the fog layer. However, Fig. 1(b and d) shows that this clustering in the CDNC value does not equate to a clustering in the LWP evolution, demonstrating that there are larger differences between the models than the predicted CDNC value.
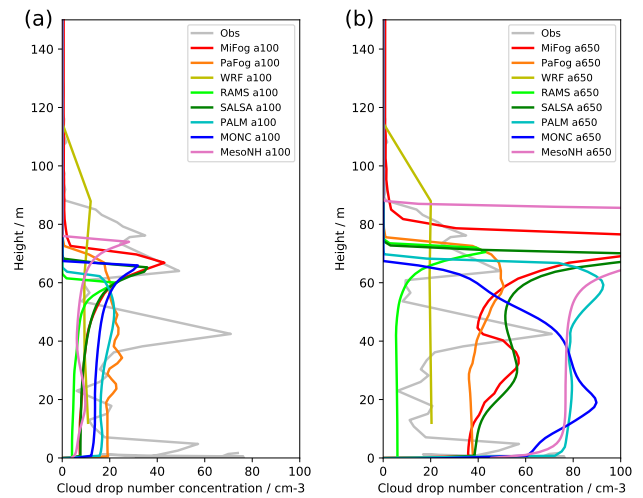
Figure 4. CDNC observed and from the aerosol processing models at 00 UTC, for (a) low aerosol, and (b) high aerosol.

It is worth briefly discussing the oscillations in LWP seen in the SCM models. This is a known feature of fog SCM simulations, and has been discussed previously by Tardif (2007). Long-wave (LW) cooling from the fog top is the key driver of the fog layer deepening. However, with the coarse vertical grid of the SCM models, the fog can only deepen in discrete units, when the top grows by a single model level. The LWP therefore erodes, by loss of moisture and heating from the surface, until such time as the fog can jump up a level, leading to a large increase in LWP as the water-vapour in the level above is available for condensation. Hence the oscillations are created. All of the SCMs with coarse vertical grids show some oscillations, although the severity of them differs significantly. By far the simulation to suffer most is Meso-NH-a, which appears to have a further complicating feedback from the microphysics. When the fog top jumps up a level, the increase in LWP triggers significant precipitation formation, which quickly removes a large amount of water from the atmosphere. This microphysical feedback does not disappear when running Meso-NH-a at higher vertical resolution,

whereas the oscillations in Meso-NH-c do (not shown), due to its use of different microphysical parametrizations.

3.2 Surface fluxes and boundary layer structure

A key feature of this fog event, and indeed many fog events, is the slow transition from a stable boundary layer with optically thin fog to a well-mixed boundary layer with optically thick fog. How this transition evolves is of key interest from a forecasting perspective, as it will determine the depth and intensity of the fog layer, and ultimately its duration into the following morning.

Interestingly, the LES models show greater variability in the surface sensible heat flux (Fig. 5a) than they did for the liquid water path. Whilst there is some hint towards the expected trend that models which are optically thickest (PALM, Meso-NH-c10) will generate a positive sensible heat flux and well-mixed fog layer first, RAMS-c10 sits as a clear outlier here generating the strongest positive sensible heat flux whilst having one of the thinnest (optically and physically) fog layers. It achieves this by forming a shallow, but well-mixed layer in which the fog exists (Fig. 6a), capped by a strong inversion. RAMS does indeed have a higher downwelling LW radiation, which would promote development of a well-mixed fog layer. However, why it keeps this layer shallow and does not grow deeper like it does in Meso-NH is interesting, suggesting lower entrainment across the inversion. The result is that RAMS has the lowest fog top of all the LES models (Fig. 7a).

The SCMs show a similar trend to the LES models, with many producing a positive surface sensible heat flux and well-mixed boundary layer structure (Figs. 5c and 6b). However those SCMs with close to zero sensible heat flux do maintain a stable potential temperature profile throughout the fog layer. As always, there are interesting outliers. The IFS in particular appears to manage a stable profile with a positive sensible heat flux. However, this is likely a consequence of the low vertical resolution, as there are only two vertical levels within the fog layer at this stage, the first of which is well-mixed and the second is stabilised by cloud top entrainment. It's also worth discussing FV3-GFS, which is the only model which produces a negative sensible heat flux. This is possibly due to its poor vertical resolution, with the lowest model level being approximately double the height of any other model, meaning the lowest level temperature is very warm relative to the surface. In its default setup, FV3-GFS also produced a very negative latent heat flux, which prevented any fog formation. Therefore a lower limit of zero on the latent heat flux was imposed in their simulations to enable fog to form.

3.3 Forecasting considerations

In terms of fog impact, particularly to the aviation sector, correctly modelling fog clearance after sunrise is key to forecasting airfield clearance time and allowing full take off/landing rates to resume. There are a number of aspects of the intercomparison which complicate the simulation of the morning transition. Firstly, the unrestricted evaporation is unrealistic for a true land-surface – soil moisture availability and resistance to evapotranspiration in grass will always result in less latent heat flux than our idealised setup will produce. Secondly, the observed surface temperature warming is representative of fog which has dissipated in reality for a number of reasons not simulated by the LES and SCMs (particularly overlying cloud cover, which is responsible for the observed increase in LWP after 08 UTC). However, comparison between how the models deal with this situation can still provide some useful insights. As shown in Figure 1, MesoNH-LES is the only model which completely dissipates the fog during the morning. Most models' fog evolution seems broadly unaffected by the increasing surface temperature and short-wave radiation, except for SALSA, where it drives a large increase in LWP. There are essentially two competing mechanisms at work here. The increase in surface temperature will drive a strong positive surface moisture flux, promoting fog development. However, direct short-wave heating of the fog layer and heating due to the rise in surface temperature and positive surface heat flux will counteract this. The consequences for fog development are therefore model dependent, based on the relative importance of these processes.

If the surface temperature was not prescribed, the key quantity driving dissipation would be the downwelling short-wave radiation (as this would drive the surface heating), which is shown in Figure 8. The figure shows that the degree of variation between models is large (over $250\,\mathrm{Wm}^{-2}$), with similar uncertainty between the LES and SCM models. To first order, the key reason for differences in the downwelling short-wave is the LWP at sunrise – the models with the highest LWP have the lowest downwelling SW and vice-versa. Optical properties of the fog appear to be much less significant here – for example comparing the UM and Meso-NH-c10 SCM simulations – Meso-NH-c10 only has a slightly smaller LWP, which offsets against its much smaller effective radius to result in almost identical downwelling SW evolution. What is clear is that there is a huge range in potential fog evolution and dissipation times driven by differences in the fog development during the night-time. Having knowledge of how realistic a model forecast of fog development through the night-time is (e.g. via real time observations) may enable a forecaster to understand how reliable the forecast for morning dissipation is. For example, real time equivalents of many of the observations presented here, such as radiosonde profiles, liquid water path measurement, surface heat, moisture and radiation fluxes, would enable a much better assessment of how the fog is developing than traditional screen-level observations can provide. Comparison of these to model diagnostics will enable an assessment of whether the model is over- or under-developing fog (optically or physically), and
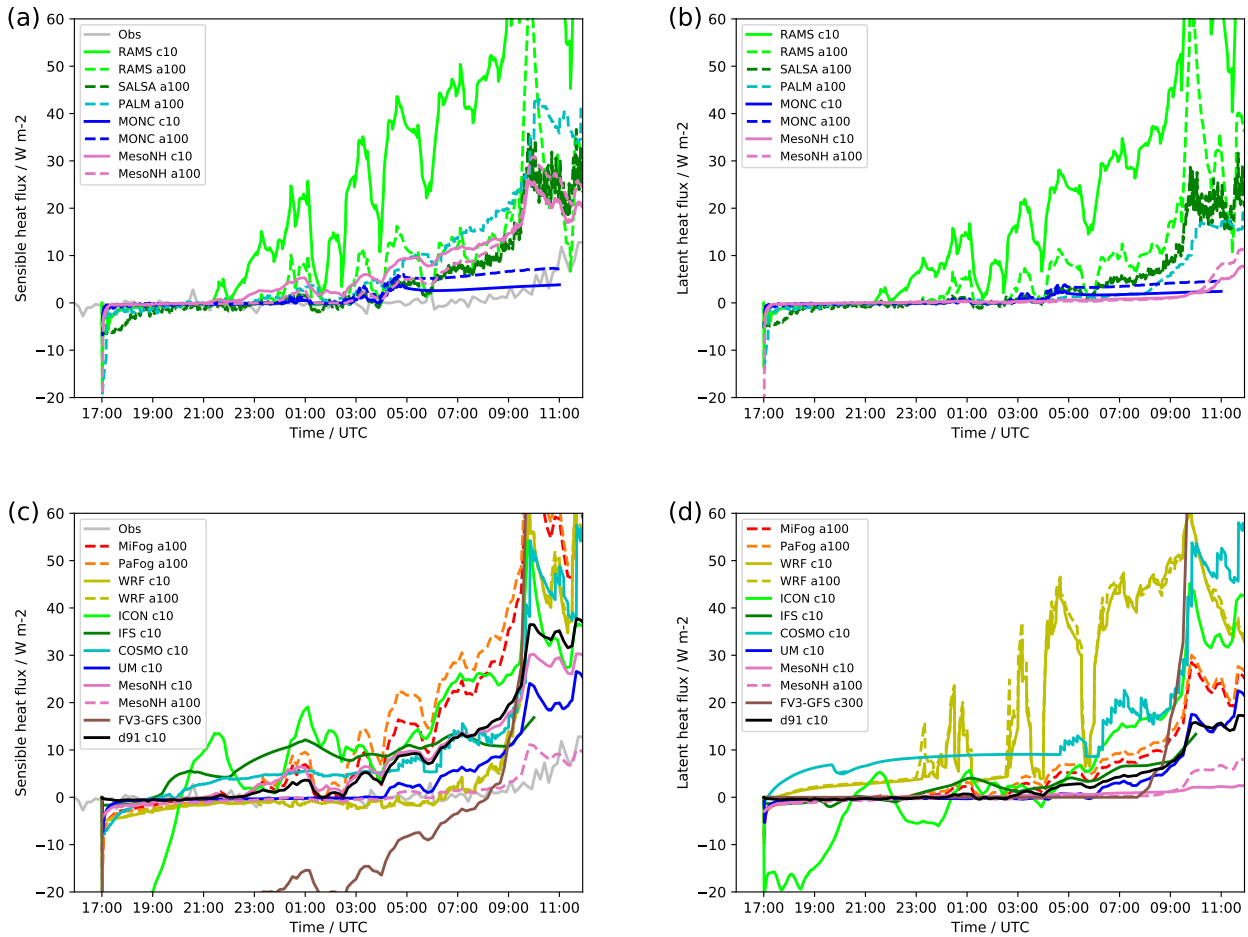
Figure 5. Sensible (left) and latent (right) heat flux observed and modelled by (top) low aerosol/CDNC LES, (bottom) low aerosol/CDNC SCMs.

therefore whether it is likely to dissipate earlier or later in the morning than forecast.

Another forecasting consideration is whether the fog will indeed dissipate, or whether it will lift into low stratus. In reality, this is governed by many factors not included in this intercomparison, such as non-local advective effects or overlying cloud cover. However, some features such as fog depth and entrainment at the fog top should be captured. Figure 9 shows the cloud base height ($q_c > 0.01$ gkg^{-1}) during the morning period for the LES and SCM models, demonstrating that there is significant variety in model simulation of this behaviour. Whilst most models keep the fog firmly on or near the ground, Meso-NH LES and COSMO SCM lift the cloud base significantly, with cloud base height exceeding 60 m (the threshold typically used by aviation for instigating low visibility procedures) by 8 UTC – 9 UTC. The difference here (and elsewhere) between Meso-NH LES and SCM is of particular interest, because the physics package of both models is identical, meaning that differences must arise

because of the lower vertical resolution in SCM, or because the 1D parametrized turbulence in the SCM is acting differently to the 3D resolved turbulence in the LES. In general, the dissipation results appear much more closely tied to individual models, rather than characteristics of the setup or development of the fog during the night. All models which provide both interactive and non-interactive aerosol setups do the same thing in both setups, and whilst for most this is to not break the fog, for Meso-NH it is to lift the fog. Similarly, for models which produce excessive LWP during the night, most do not break it whilst COSMO lifts it. A more focussed intercomparison on the dissipation phase is likely required to fully understand this model-dependent behaviour and link it to physical processes.

Finally, we discuss some of the typical metrics used by decision makers when forecasting fog events. Figure 10(a) shows the visibility as predicted by all models incorporating a visibility parametrization. The visibility parametrization is model dependent, with those used listed in Table 4. Some
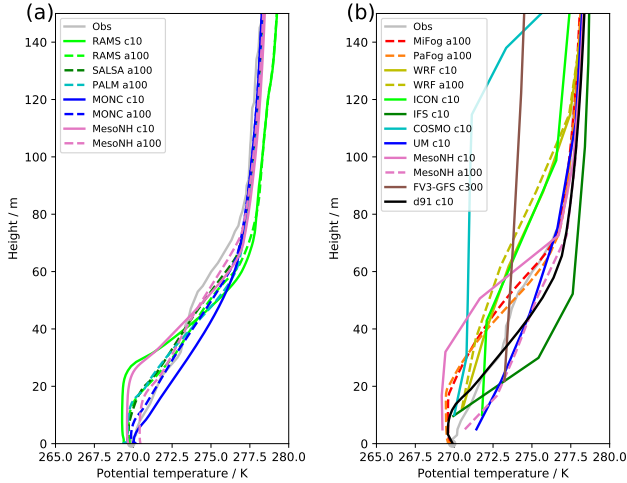
Figure 6. Potential temperature observed and simulated by (a) the low aerosol/CDNC LES models, and (b) the low aerosol/CDNC SCMs at 00 UTC.
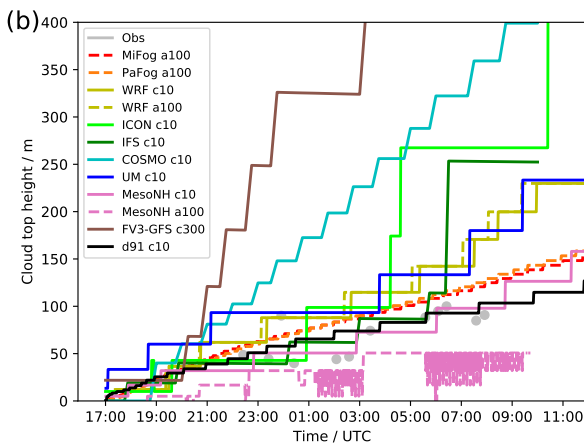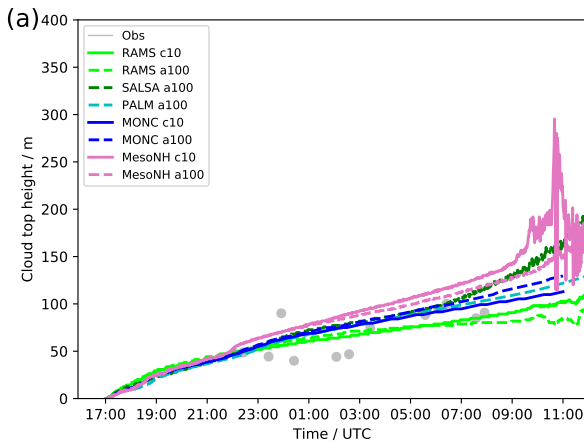
Figure 7. Fog top height observed and modelled by (a) low aerosol/CDNC LES, (b) low aerosol/CDNC SCMs.
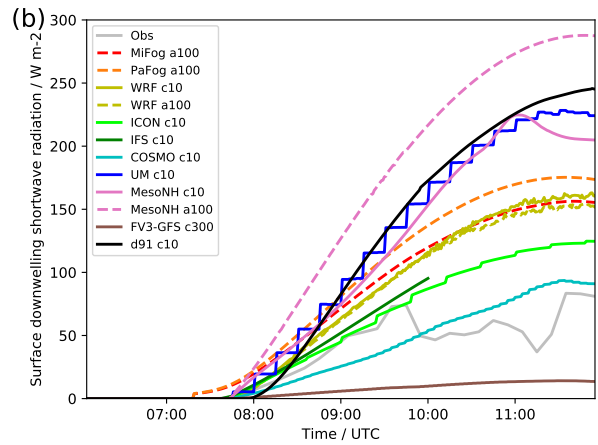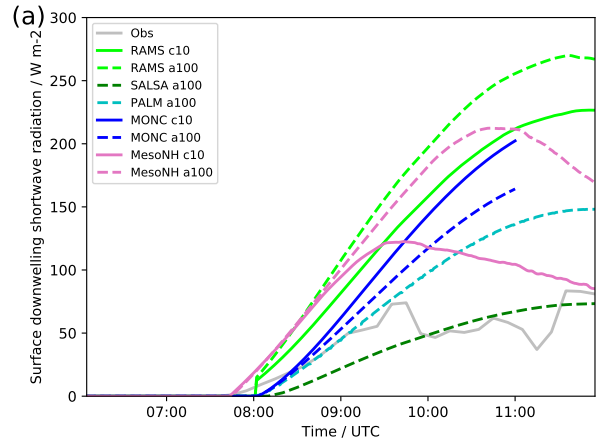
Figure 8. Surface downwelling short-wave radiation observed and modelled by (a) low aerosol/CDNC LES, (b) low aerosol/CDNC SCMs.

parametrizations utilise a direct empirical link between cloud water content and visibility, whilst others attempt to calculate the extinction coefficient directly based on the aerosol distribution and atmospheric humidity. Models where the vertical resolution does not give a grid-level at the screen-level height (1.5–3 m), either use values at the lowest model level (Tab 4) or first produce input variables to the visibility parametrization at this level via interpolation. Given the differences seen elsewhere in the fog evolution, the level of agreement between models here is somewhat surprising. Most models are forecasting visibility in the 100-300 m range for most of the night, in line with observations. IFS and PALM are forecasting slightly larger visibilities (≈500 m), but still below the thresholds typically used by aviation decision makers (600 m), whilst only Meso-NH produces visibilities below 100 m. Most models also retain low visibilities well into the morning period, with only Meso-NH, IFS and eventually the UM forecasting a clearance in this metric. The consistent be-
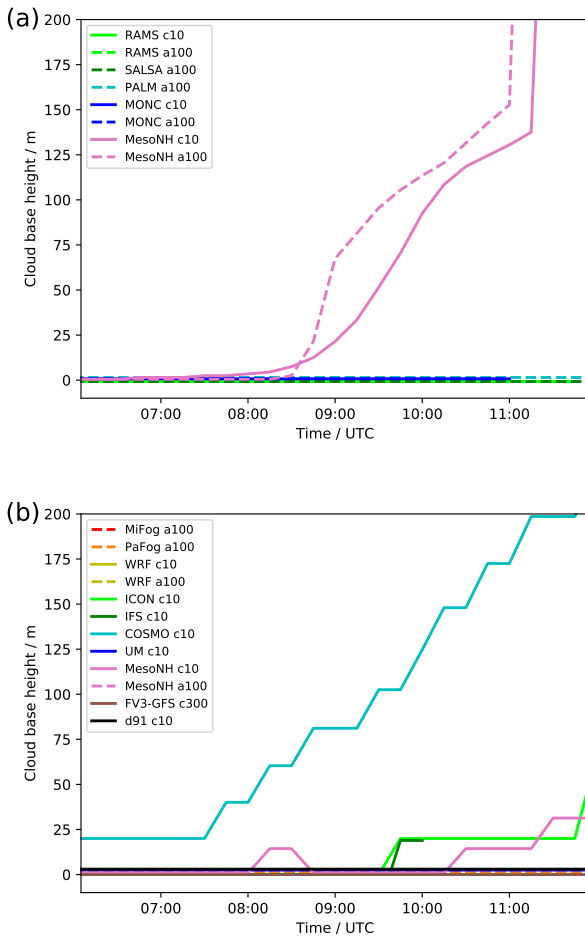
Figure 9. Cloud base height modelled by (a) low aerosol/CDNC LES, (b) low aerosol/CDNC SCMs.
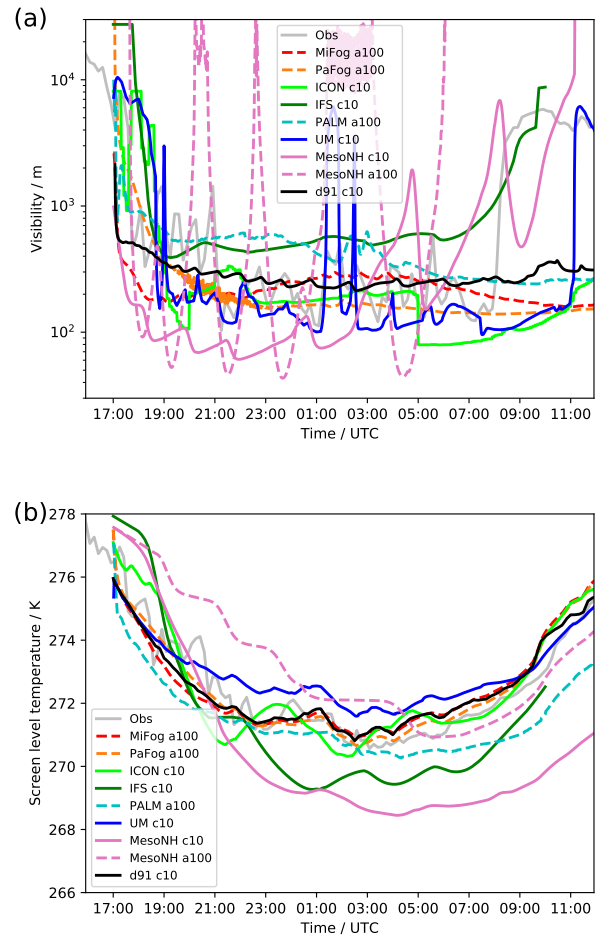
Figure 10. (a) Visibility, and (b) screen level temperature, observed and predicted by all models including a specific visibility parametrization.

haviour may, in part, be due to the tight linkage between screen-level and surface variables in many models, as with the surface temperature prescribed, the screen-level temperature does not deviate far from the observations (Fig 10b). However, it also raises caution against the use and interpretation of such variables, if they can seemingly produce such similar results despite such obvious differences in the actual simulation of fog within the models. To truly understand and interpret an NWP fog forecast requires much more than simply looking at the predicted visibility, especially in more marginal cases than this one.

Table 4 shows for all models the onset and dissipation time of the fog event, and the maximum height reached by the fog layer. This summarises many of the themes discussed so far in the paper. The initiation of fog is handled well by all models, with the initiation happening between 17 and 18 UTC in all but 2 of the models. Many models show that low visibility (LVP) occurs some time after fog onset, demonstrating that the models are able to capture an initial period of thin

fog where visibility remains good. The dissipation phase is much poorer, with most models persisting fog until the end of the simulation. Only a minority of models break the fog during the morning period, and with no consistency in how this is done – some lifting it into stratus whilst others clear it entirely. Whilst a few models do thin the fog sufficiently for LVP to end, it would clearly be very difficult to provide guidance to customers based on this ensemble set. The mean fog depth simulated by the SCMs is approximately 100 m higher than that from the LES, and at the very top end of the LES range. This is symptomatic of the SCM behaviour in producing fog which is too thick, a characteristic that will likely lead to fog persisting for too long into the daytime.

	Fog onset	LVP start	Fog dissipation	LVP end	Max fog top (m)	Visibility parametrization
Observations		17:45		08:04	≈100**	
MiFog SCM a100	17:00	17:11	>12	>12	153	Physical: Bott (2021)
PaFog SCM a100	17:15	18:25	>12	>12	159	Physical: Bott (2021)
WRF SCM c10	17:30		>12		230	
WRF SCM a100	17:30		>12		230	
RAMS LES c10	17:30		>12		110	
RAMS LES a100	17:30		>12		95	
ICON SCM c10	17:30	18:49	11:45	>12	503	Empirical: Kunkel (1984)
IFS SCM c10	17:52	18:37	>12	06:37	253	Physical[†]: Gultepe et al. (2006)
SALSA LES a100	17:10		>12		196	
COSMO SCM c10	19:00		08:00		489	
PALM LES a100	17:00	19:09	>12	>12	130	Empirical: Gultepe et al. (2006)
UM SCM c10	17:01	18:41	>12	11:08	233	Physical: Clark et al. (2008)
MONC LES c10	17:30		>12		113	
MONC LES a100	17:30		>12		129	
MesoNH SCM c10	17:15	17:15	>12	09:19	158	Empirical[†]: Kunkel (1984)
MesoNH SCM a100	17:45	17:45	06:00	05:30	51	Physical[†]: similar to Bott (2021)
MesoNH LES c10	17:30		09:15		295	
MesoNH LES a100	17:30		08:45		271	
FV3-GFS SCM c300	20:15		>12		622	
d91 SCM c10	17:04	17:10	>12	>12	127	Empirical: Kunkel (1984)
LES mean	17:23		09:00*		167	
LES range	0:30		0:30*		200	
SCM mean	17:44	17:59	08:35*	08:08*	267	
SCM range	3:15	1:39	5:45*	5:38*	571	

Table 4. Selected forecasting metrics for each model, as observed, and the mean and range of results for the LES and SCM models combined. Fog onset/dissipation is defined by liquid water below 60 m, whilst typical airfield low visibility procedures (LVP) are defined by visibility <600 m and cloud base <60 m. '>12' denotes models which did not dissipate fog by the end of the simulation. *Dissipation statistics are only calculated from the models which dissipated fog during the morning. **Recorded around 08 UTC just before the fog dissipated. [†]Parametrizations are applied at the lowest model level (Tab 3) rather than the screen level.

4   Microphysics Parametrization Sensitivity

To explore some of the themes and relationships shown in Section 3.1, in this section we focus on 2 SCMs (COSMO and UM) and 1 LES (MONC), modifying several
5 parametrizations to confirm the speculated reasons for fog differences. The first and most simple test, using the UM, is to switch off cloud droplet sedimentation entirely (similar to COSMO, FV3-GFS or IFS). This is shown in Figure 11.

The removal of cloud droplet sedimentation leads to large
10 increases in the liquid water path, for both CDNC values. Clearly the presence or absence of cloud drop sedimentation is more important than the prescription of CDNC value. This also confirms why models which do not represent this process produce a fog layer which is too thick.

15 Whilst implementing cloud droplet sedimentation in models which do not have it is ultimately the most physically realistic way of improving fog simulation, we can also investigate, using COSMO, how simulations might be improved with the parametrizations at hand. The autocon-
20 version in COSMO (Seifert and Beheng, 2001) is proportional to the 4th power of cloud water content, and therefore produces very little autoconversion at low water contents. Re-
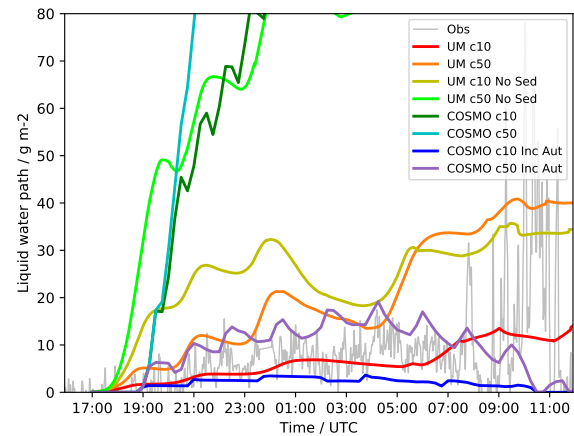
Figure 11. Liquid water path observed and modelled with low and high CDNC values, from the UM with or without cloud droplet sedimentation, and COSMO with low and high autoconversion rates (see caption).

ducing the power (to 3.1) allows the autoconversion rate to be increased at low water contents. As shown in Figure 11, the consequence of this is a much improved fog simulation, again confirming that the rate of water loss from the atmo-
5 sphere is the dominant mechanism governing the fog LWP. This also shows why IFS, which uses Khairoutdinov and Kogan (2000) autoconversion (power 2.47) is able to produce lower and more realistic LWP evolution without cloud droplet sedimentation. It is worth clarifying again that this is
10 not a realistic model improvement we would suggest implementing – fog droplets are small and collision-coalescence is rare, therefore autoconversion should not be happening.

For models which do simulate cloud droplet sedimentation, how sensitive is the fog development to the precise de-
15 tails of the parametrization? This is explored with the MONC LES, by varying the shape parameter, μ, used in the cloud droplet size distribution:

$$N(D) = N_0 D^\mu e^{-\lambda D}, \qquad (1)$$

where N is the number of drops of diameter D, N_0 is the
20 intercept parameter and λ is the slope parameter. Miles et al. (2000) have shown that μ in the range 2-5 is most commonly found in stratiform clouds, but values in the range 0-25 have been found in observations. The default value used in MONC is $\mu = 2.5$, and Figure 12 shows a sensitivity study varying μ
25 between 0 and 10.
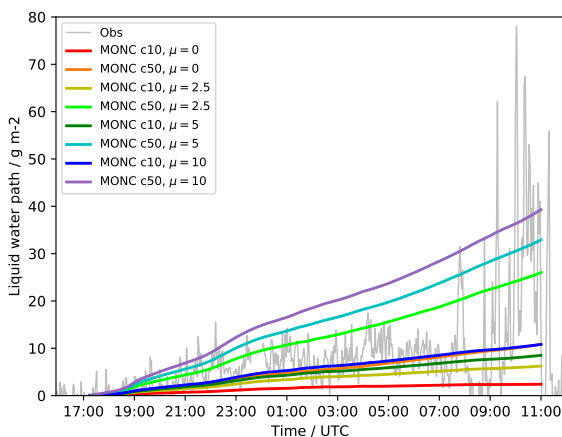
Figure 12. Liquid water path observed and modelled by MONC with low and high CDNC values, with varied values of the shape parameter μ (see caption).

Once again, this relatively minor change to part of the microphysical parametrization can have a similar sized effect on fog evolution to the prescribed CDNC value, showing the importance of fundamental parametrization development. It's
30 also interesting to note that with the reduction of μ, which increases droplet sedimentation rates, it is actually possible to produce a fog layer which is too thin – no other model has

shown this so far. This acts to highlight why even when all processes are represented within a model, large differences in fog evolution can still be seen because the fog evolution is
35 so sensitive to small parametrization changes.

This section has shown that even for a highly constrained scenario, the microphysics of fog remains a very uncertain process. We could, for example, recommend that future field campaigns focus on ascertaining with better accuracy
40 the parameters of bulk microphysics parametrizations (for example μ). However, existing observations show that frequently size distributions are bimodal in nature (Wendisch et al., 1998; Price, 2011), and therefore we should question whether microphysics parametrizations imposing a Gamma
45 distribution are even the appropriate tool for fog simulation. Bin microphysics parametrizations (such as that employed in SALSA or MiFog) offer a better ability to simulate the evolution of the size distribution, and certainly these models are among the best performing in this intercomparison.
50 Recently, Schwenkel and Maronga (2020) demonstrated the use of a Lagrangian cloud model (LCM) for fog simulation, and found (consistent with this work) that the LCM tended to produce greater sedimentation rates and lower liquid water paths than a bulk scheme, due to its evolution of the size dis-
55 tribution. However Bin schemes and LCMs are likely to be prohibitively expensive for operational implementation, and therefore how to best represent this behaviour in operational models remains an open question. They also contain many more degrees of freedom, and thus it is important that future
60 observational campaigns focus not just on the mean value of microphysical parameters, but also the time and space variability of the full size distribution, to allow accurate evaluation of Bin schemes and LCMs.

5 Conclusions   65

If nothing else, this paper has highlighted why fog remains such a difficult forecasting challenge. The level of comparability between our most detailed process models – LES – is much lower than has been seen in previous intercomparison studies of other boundary-layer or cloud regimes (Beare
70 et al., 2006; van der Dussen et al., 2013). This is largely due to the huge role microphysics plays in fog development, and uncertainties inherent in the representation of a process which is still entirely parametrized in LES. However, there were also strong differences seen in the surface fluxes and
75 turbulent structure within the LES models. Whilst throughout the bulk of the fog layer the simulations were well enough resolved, near the surface the sub-filter scale flux clearly becomes dominant and provides an additional source of uncertainty not seen with higher-level clouds. This effectively
80 means that LES cannot be considered an adequate baseline (or truth) against which to compare NWP models. Therefore our first recommendation must be for continued investment in observational understanding of real fog events, particu-

larly to understand the high-frequency (in time and space) variability that exists in fog. This must be linked to continued development of LES models to a state where they can provide an adequate substitute for real observations.

For the SCMs, it is clear that improvements have been made since the previous intercomparison of Bergot et al. (2007), as a very good consistency between models in the fog onset phase was achieved. However, after onset the NWP-SCMs are of highly variable quality, but there appears to be a general trend for over development of fog, i.e. models produce fog which is too physically and optically thick, too quickly. There are some simple improvements (such as the inclusion of cloud droplet sedimentation) which should be applied to some models, but further improvements could require some significant parametrization development. This work has given some guidance as to where that work should be focussed, as we have shown that fundamental parametrizations (such as cloud microphysics) are as uncertain and important in simulating fog development as implementing new feedback processes (such as aerosol interaction). However, there are still fundamental questions on the interaction between cloud, radiation and turbulence in fog which require further investigation. Additionally, these conclusions are only drawn for a single case, and therefore it is important to continue the intercomparison of models on a wider range of cases, in different geographic locations and with different forcings.

Regarding forecasting applications, this work has shown that the early stages of fog development crucially impact its decay phase the following morning. This suggests that if real-time comparison of NWP forecast to observations can be conducted during the night-time, it could be used to help determine how accurate the NWP dissipation forecasts will be, allowing them to be manually adapted to give the best guidance to customers. Success has been seen with techniques like this in the past (Bergot, 2007), and with new and emerging observational platforms (such as UAVs), more detailed measurements of the fog properties (e.g. real-time droplet spectra) could further improve customer guidance.

Data availability. The data is available from the authors upon request.

Author contributions. IB analysed the submitted results and wrote the manuscript. IB, WA, RB, AB, LD, RF, TG, EG, AH, AI, IK, JS and GS ran the model simulations. All authors contributed to the discussion, understanding and presentation of results, and preparation of the manuscript.

Competing interests. The authors declare that they have no conflict of interest.

Acknowledgements. WA thanks Greg Thompson of NCAR for help in understanding and setting parameters in the Thompson microphysics schemes in WRF. JS was supported by the Hans Ertel Centre for Weather Research of DWD (The Atmospheric Boundary Layer in Numerical Weather Prediction) grant number 4818DWDP4. RB was supported by MeteoSwiss (project number 123001738). This work used resources of the Deutsches Klimarechenzentrum (DKRZ) granted by its Scientific Steering Committee (WLA) under project ID bb1096. IK and SR acknowledge the Horizon 2020 Research and Innovation Programme (grant no. 821205).

References

Ahlgrimm, M. and Forbes, R.: Improving the representation of low clouds and drizzle in the ECMWF model based on ARM observations from the Azores, Mon. Weather Rev., 142, 668–685, 2014.

Angevine, W. M., Olson, J., Kenyon, J., Gustafson, W. I., Endo, S., Suselj, K., and Turner, D. D.: Shallow Cumulus in WRF Parameterizations Evaluated against LASSO Large-Eddy Simulations, Mon. Weather Rev., 146, 4303–4322, https://doi.org/10.1175/MWR-D-18-0115.1, 2018.

Baldauf, M., Seifert, A., Förstner, J., Majewski, D., Raschendorfer, M., and Reinhardt, T.: Operational Convective-Scale Numerical Weather Prediction with the COSMO Model: Description and Sensitivities, Mon. Weather Rev., 139, 3887–3905, https://doi.org/10.1175/MWR-D-10-05013.1, 2011.

Bašták Ďurán, I., Köhler, M., Eichhorn-Müller, A., Maurer, V., Schmidli, J., Schomburg, A., Klocke, D., Göcke, T., Schäfer, S., Schlemmer, L., and Dewani, N.: The ICON Single-Column Mode, Atmosphere, 12, 906, https://doi.org/10.3390/atmos12070906, 2021.

Beare, R. J., MacVean, M. K., Holtslag, A. A. M., Cuxart, J., Esau, I., Golaz, J.-C., Jimenez, M. A., Khairoutdinov, M., Kosovic, B., Lewellen, D., Lund, T. S., Lundquist, J. K., McCabe, A., Moene, A. F., Noh, Y., Raasch, S., and Sullivan, P.: An Intercomparison of Large-Eddy Simulations of the Stable Boundary Layer, Boundary-Layer Meteorol., 118, 247–272, https://doi.org/10.1007/s10546-004-2820-6, 2006.

Bergot, T.: Quality assessment of the Cobel-Isba numerical forecast system of fog and low clouds, Pure Appl. Geophys., 164, 1265–1282, https://doi.org/10.1007/978-3-7643-8419-7_10, 2007.

Bergot, T., Terradellas, E., Cuxart, J., Mira, A., Liechti, O., Mueller, M., and Nielsen, N. W.: Intercomparison of Single-Column Numerical Models for the Prediction of Radiation Fog, J. Appl. Meteorol. Climatol., 46, 504–521, https://doi.org/10.1175/JAM2475.1, 2007.

Bott, A.: Comparison of a spectral microphysics and a two-moment cloud scheme: Numerical simulation of a radiation fog event, Atmos. Res., 262, 105787, https://doi.org/10.1016/j.atmosres.2021.105787, 2021.

Bott, A. and Trautmann, T.: PAFOG – a new efficient forecast model of radiation fog and low-level stratiform clouds, Atmos. Res., 64, 191–203, https://doi.org/10.1016/S0169-8095(02)00091-1, 2002.

Bott, A., Sievers, U., and Zdunkowski, W.: A Radiation Fog Model with a Detailed Treatment of the Interaction between Radiative Transfer and Fog Microphysics, J.

Atmos. Sci., 47, 2153–2166, https://doi.org/10.1175/1520-0469(1990)047<2153:ARFMWA>2.0.CO;2, 1990.

Boutle, I., Price, J., Kudzotsa, I., Kokkola, H., and Romakkaniemi, S.: Aerosol-fog interaction and the transition to well-mixed radiation fog, Atmos. Chem. Phys., 18, 7827–7840, https://doi.org/10.5194/acp-18-7827-2018, 2018.

Bush, M., Allen, T., Bain, C., Boutle, I., Edwards, J., Finnenkoetter, A., Franklin, C., Hanley, K., Lean, H., Lock, A., Manners, J., Mittermaier, M., Morcrette, C., North, R., Petch, J., Short, C., Vosper, S., Walters, D., Webster, S., Weeks, M., Wilkinson, J., Wood, N., and Zerroukat, M.: The first Met Office Unified Model–JULES Regional Atmosphere and Land configuration, RAL1, Geosci. Model Dev., 13, 1999–2029, https://doi.org/10.5194/gmd-13-1999-2020, 2020.

Buzzi, M., Rotach, M. W., Holtslag, M., and Holtslag, A. A.: Evaluation of the COSMO-SC turbulence scheme in a shear-driven stable boundary layer, Meteor. Z., 20, 335–350, https://doi.org/10.1127/0941-2948/2011/0050, 2011.

Clark, P. A., Harcourt, S. A., Macpherson, B., Mathison, C. T., Cusack, S., and Naylor, M.: Prediction of visibility and aerosol within the operational Met Office Unified Model. I: Model formulation and variational assimilation, Q. J. R. Meteorol. Soc., 134, 1801–1816, https://doi.org/10.1002/qj.318, 2008.

Cook, A. J. and Tanner, G.: The cost of passenger delay to airlines in Europe - consultation document, https://westminsterresearch.westminster.ac.uk/item/q4qq5/the-cost-of-passenger-delay-to-airlines-in-europe-consultation-document, 2015.

Cotton, W. R., Pielke Sr., R. A., Walko, R. L., Liston, G. E., Tremback, C. J., Jiang, H., McAnelly, R. L., Harrington, J. Y., Nicholls, M. E., Carrio, G. G., and McFadden, J. P.: RAMS 2001: Current status and future directions, Meteorol. Atmos. Phys., 82, 5–29, https://doi.org/10.1007/s00703-001-0584-9, 2003.

Cuxart, J., Holtslag, A. A. M., Beare, R. J., Bazile, E., Beljaars, A., Cheng, A., Conangla, L., Ek, M., Freedman, F., Hamdi, R., Kerstein, A., Kitagawa, H., Lenderink, G., Lewellen, D., Mailhot, J., Mauritsen, T., Perov, V., Schayes, G., Steeneveld, G.-J., Svensson, G., Taylor, P., Weng, W., Wunsch, S., and Xu, K.-M.: Single-Column Model Intercomparison for a Stably Stratified Atmospheric Boundary Layer, Boundary-Layer Meteorol., 118, 273–303, https://doi.org/10.1007/s10546-005-3780-1, 2006.

Dearden, C., Hill, A., Coe, H., and Choularton, T.: The role of droplet sedimentation in the evolution of low-level clouds over southern West Africa, Atmos. Chem. Phys., 18, 14 253–14 269, https://doi.org/10.5194/acp-18-14253-2018, 2018.

Duynkerke, P. G.: Radiation Fog: A Comparison of Model Simulation with Detailed Observations, Mon. Weather Rev., 119, 324–341, https://doi.org/10.1175/1520-0493(1991)119<0324:RFACOM>2.0.CO;2, 1991.

Firl, G., Carson, L., Bernardet, L., Heinzeller, D., and Harrold, M.: Common Community Physics Package Single Column Model v4.0 User and Technical Guide, https://dtcenter.org/GMTB/v4.0/scm-ccpp-guide-v4.pdf, 2020.

Gultepe, I., Muller, M. D., and Boybeyi, Z.: A New Visibility Parameterization for Warm-Fog Applications in Numerical Weather Prediction Models, J. Appl. Meteorol. Climatol., 45, 1469–1480, https://doi.org/10.1175/JAM2423.1, 2006.

Gultepe, I., Sharman, R., Williams, P. D., Zhou, B., Ellrod, G., Minnis, P., Trier, S., Griffin, S., Yum, S. S., Gharabaghi, B., Feltz,

W., Temimi, M., Pu, Z., Storer, L. N., Kneringer, P., Weston, M. J., Chuang, H.-y., Thobois, L., Dimri, A. P., Dietz, S. J., Franca, G. B., Almeida, M. V., and Neto, F. L. A.: A Review of High Impact Weather for Aviation Meteorology, Pure Appl. Geophys., 176, 1869–1921, https://doi.org/10.1007/s00024-019-02168-6, 2019.

Hewson, T.: Use and Verification of ECMWF Products in Member and Co-operating States (2018), ECMWF Technical Memoranda, https://doi.org/10.21957/jgz6nh0uc, 2019.

Hill, A. A., Shipway, B. J., and Boutle, I. A.: How sensitive are aerosol-precipitation interactions to the warm rain representation?, J. Adv. Model. Earth Syst., 7, 987–1004, https://doi.org/10.1002/2014MS000422, 2015.

Khairoutdinov, M. and Kogan, Y.: A New Cloud Physics Parameterization in a Large-Eddy Simulation Model of Marine Stratocumulus, Mon. Weather Rev., 128, 229–243, 2000.

Kulkarni, R., Jenamani, R. K., Pithani, P., Konwar, M., Nigam, N., and Ghude, S. D.: Loss to Aviation Economy Due to Winter Fog in New Delhi during the Winter of 2011-2016, Atmosphere, 10, 198, https://doi.org/10.3390/atmos10040198, 2019.

Kunkel, B. A.: Parameterization of Droplet Terminal Velocity and Extinction Coefficient in Fog Models, J. Appl. Meteorol. Climatol., 23, 34–41, https://doi.org/10.1175/1520-0450(1984)023<0034:PODTVA>2.0.CO;2, 1984.

Lac, C., Chaboureau, J.-P., Masson, V., Pinty, J.-P., Tulet, P., Escobar, J., Leriche, M., Barthe, C., Aouizerats, B., Augros, C., Aumond, P., Auguste, F., Bechtold, P., Berthet, S., Bielli, S., Bosseur, F., Caumont, O., Cohard, J.-M., Colin, J., Couvreux, F., Cuxart, J., Delautier, G., Dauhut, T., Ducrocq, V., Filippi, J.-B., Gazen, D., Geoffroy, O., Gheusi, F., Honnert, R., Lafore, J.-P., Lebeaupin Brossier, C., Libois, Q., Lunet, T., Mari, C., Maric, T., Mascart, P., Mogé, M., Molinié, G., Nuissier, O., Pantillon, F., Peyrillé, P., Pergaud, J., Perraud, E., Pianezze, J., Redelsperger, J.-L., Ricard, D., Richard, E., Riette, S., Rodier, Q., Schoetter, R., Seyfried, L., Stein, J., Suhre, K., Taufour, M., Thouron, O., Turner, S., Verrelle, A., Vié, B., Visentin, F., Vionnet, V., and Wautelet, P.: Overview of the Meso-NH model version 5.4 and its applications, Geosci. Model Dev., 11, 1929–1969, https://doi.org/10.5194/gmd-11-1929-2018, 2018.

Leung, A. C. W., Gough, W. A., and Butler, K. A.: Changes in Fog, Ice Fog, and Low Visibility in the Hudson Bay Region: Impacts on Aviation, Atmosphere, 11, 186, https://doi.org/10.3390/atmos11020186, 2020.

Maronga, B., Banzhaf, S., Burmeister, C., Esch, T., Forkel, R., Fröhlich, D., Fuka, V., Gehrke, K. F., Geletič, J., Giersch, S., Gronemeier, T., Groß, G., Heldens, W., Hellsten, A., Hoffmann, F., Inagaki, A., Kadasch, E., Kanani-Sühring, F., Ketelsen, K., Khan, B. A., Knigge, C., Knoop, H., Krč, P., Kurppa, M., Maamari, H., Matzarakis, A., Mauder, M., Pallasch, M., Pavlik, D., Pfafferott, J., Resler, J., Rissmann, S., Russo, E., Salim, M., Schrempf, M., Schwenkel, J., Seckmeyer, G., Schubert, S., Sühring, M., von Tils, R., Vollmer, L., Ward, S., Witha, B., Wurps, H., Zeidler, J., and Raasch, S.: Overview of the PALM model system 6.0, Geosci. Model Dev., 13, 1335–1372, https://doi.org/10.5194/gmd-13-1335-2020, 2020.

Martin, G. M., Johnson, D. W., and Spice, A.: The Measurement and Parameterization of Effective Radius of Droplets in Warm Stratocumulus Clouds, J. At-

mos. Sci., 51, 1823–1842, https://doi.org/10.1175/1520-0469(1994)051<1823:TMAPOE>2.0.CO;2, 1994.

Miles, N. L., Verlinde, J., and Clothiaux, E. E.: Cloud Droplet Size Distributions in Low-Level Stratiform Clouds, J. Atmos. Sci., 57, 295–311, https://doi.org/10.1175/1520-0469(2000)057<0295:CDSDIL>2.0.CO;2, 2000.

Neggers, R. A. J., Ackerman, A. S., Angevine, W. M., Basile, E., Beau, I., Blossey, P. N., Boutle, I. A., de Bruijn, C., Cheng, A., van der Dussen, J., Fletcher, J., dal Gesso, S., Jam, A., Kawai, H., Kumar, S., Larson, V. E., Lefebvre, M.-P., Lock, A. P., Meyer, N. R., de Roode, S. R., de Rooy, W., Sandu, I., Xiao, H., and Xu, K.-M.: Single-column model simulations of subtropical marine boundary-layer cloud transitions under weakening inversions, J. Adv. Model. Earth Syst., 9, 2385–2412, https://doi.org/10.1002/2017MS001064, 2017.

Price, J.: Radiation Fog. Part I: Observations of Stability and Drop Size Distributions, Boundary-Layer Meteorol., 139, 167–191, https://doi.org/10.1007/s10546-010-9580-2, 2011.

Price, J., Lane, S., Boutle, I., Smith, D., Bergot, T., Lac, C., Duconge, L., McGregor, J., Kerr-Munslow, A., Pickering, M., and Clark, R.: LANFEX: a field and modelling study to improve our understanding and forecasting of radiation fog, Bull. Amer. Meteor. Soc., 99, 2061–2077, https://doi.org/10.1175/BAMS-D-16-0299.1, 2018.

Schwenkel, J. and Maronga, B.: Towards a Better Representation of Fog Microphysics in Large-Eddy Simulations Based on an Embedded Lagrangian Cloud Model, Atmosphere, 11, 466, https://doi.org/10.3390/atmos11050466, 2020.

Seifert, A. and Beheng, K. D.: A double-moment parameterization for simulating autoconversion, accretion and selfcollection, Atmos. Res., 59-60, 265–281, https://doi.org/10.1016/S0169-8095(01)00126-0, 2001.

Tardif, R.: The Impact of Vertical Resolution in the Explicit Numerical Forecasting of Radiation Fog: A Case Study, Pure Appl. Geophys., 164, 1221–1240, https://doi.org/10.1007/s00024-007-0216-5, 2007.

Tonttila, J., Maalick, Z., Raatikainen, T., Kokkola, H., Kühn, T., and Romakkaniemi, S.: UCLALES–SALSA v1.0: a large-eddy model with interactive sectional microphysics for aerosol, clouds and precipitation, Geosci. Model Dev., 10, 169–188, https://doi.org/10.5194/gmd-10-169-2017, 2017.

van der Dussen, J. J., de Roode, S. R., Ackerman, A. S., Blossey, P. N., Bretherton, C. S., Kurowski, M. J., Lock, A. P., Neggers, R. A. J., Sandu, I., and Siebesma, A. P.: The GASS/EUCLIPSE model intercomparison of the stratocumulus transition as observed during ASTEX: LES results, J. Adv. Model. Earth Syst., 5, 483–499, https://doi.org/10.1002/jame.20033, 2013.

Vié, B., Ducongé, L., Lac, C., Bergot, T., and Price, J.: LES simulations of LANFEX IOP1 radiative fog event: prognostic vs. diagnostic supersaturation for CCN activation, Q. J. R. Meteorol. Soc., in prep., 2021.

Wendisch, M., Mertes, S., Heintzenberg, J., Wiedensohler, A., Schell, D., Wobrock, W., Frank, G., Martinsson, B. G., Fuzzi, S., Orsi, G., Kos, G., and Berner, A.: Drop size distribution and LWC in Po Valley fog, Contr. Atmos. Phys., 71, 87–100, 1998.